

1 **TITLE**

2 Biominalisation plasticity and environmental heterogeneity predict geographic resilience
3 patterns of foundation species to future change

4

5 **Running title**

6 Shell plasticity predicts resilience

7

8 **List of authors**

9 Luca Telesca,^{1,2} Lloyd S. Peck,² Trystan Sanders,³ Jakob Thyrring,^{2,4} Mikael K. Sejr,^{5,6} Elizabeth
10 M. Harper¹

11

12 **Institutional affiliations**

13 ¹ Department of Earth Sciences, University of Cambridge, CB2 3EQ Cambridge, UK.

14 ² British Antarctic Survey, CB3 0ET Cambridge, UK.

15 ³ GEOMAR Helmholtz Centre for Ocean Research, 24105 Kiel, Germany.

16 ⁴ Department of Zoology, University of British Columbia, V6T 1Z4, Vancouver, BC, Canada

17 ⁵ Department of Bioscience, Arctic Research Centre, Aarhus University, 8000 Aarhus C,

18 Denmark.

19 ⁶ Department of Bioscience, Marine Ecology, Aarhus University, 8600 Silkeborg, Denmark.

20

21 **Contact Information**

22 Luca Telesca, email: lt401@cam.ac.uk, phone: +44 (0) 1223 33408

23 Elizabeth M. Harper, email: emh21@cam.ac.uk, phone: +44 (0) 1223 333428

24 **ABSTRACT**

25 Although geographic patterns of species' sensitivity to environmental changes are defined by
26 interacting multiple stressors, little is known about compensatory processes shaping regional
27 differences in organismal vulnerability. Here, we examine large-scale spatial variations in
28 biomineralisation under heterogeneous environmental gradients of temperature, salinity, and
29 food availability across a 30° latitudinal range (3,334 km), to test whether plasticity in calcareous
30 shell production and composition, from juveniles to large adults, mediates geographic patterns of
31 resilience to climate change in critical foundation species, the mussels *Mytilus edulis* and *M.*
32 *trossulus*. We find shell calcification decreased towards high latitude, with mussels producing
33 thinner shells with a higher organic content in polar than temperate regions. Salinity was the best
34 predictor of within-region differences in mussel shell deposition, mineral and organic
35 composition. In polar, subpolar, and Baltic low-salinity environments, mussels produced thin
36 shells with a thicker external organic layer (periostracum), and an increased proportion of calcite
37 (prismatic layer, as opposed to aragonite) and organic matrix, providing potentially higher
38 resistance against dissolution in more corrosive waters. Conversely, in temperate, higher-salinity
39 regimes, thicker, more calcified shells with a higher aragonite (nacreous layer) proportion were
40 deposited, which suggests enhanced protection under increased predation pressure. Interacting
41 effects of salinity and food availability on mussel shell composition predict the deposition of a
42 thicker periostracum and organic-enriched prismatic layer under forecasted future environmental
43 conditions, suggesting a capacity for increased protection of high-latitude populations from
44 ocean acidification. These findings support biomineralisation plasticity as a potentially
45 advantageous compensatory mechanisms conferring *Mytilus* species a protective capacity for
46 quantitative and qualitative trade-offs in shell deposition as a response to regional alterations of

47 abiotic and biotic conditions in future environments. Our work illustrates that compensatory
48 mechanisms, driving plastic responses to the spatial structure of multiple stressors, can define
49 geographic patterns of unanticipated species resilience to global environmental change.

50

51 **Keywords**

52 Climate change, *Mytilus*, calcification, biomineralisation, resistance, ocean acidification,
53 compensatory mechanisms, multiple stressors

54 **INTRODUCTION**

55 Unprecedented global environmental changes are driving scientists towards increased efforts to
56 investigate the mechanisms underlying geographic variation in biotic responses to future
57 environmental conditions (Nagelkerken & Connell, 2015; Urban et al., 2016). However, our
58 ability to predict changes to species and ecosystems in response to climate change remains
59 limited (Kroeker, Kordas, & Harley, 2017). Current projections are severely constrained by
60 heterogeneous patterns of ocean warming and acidification (Gattuso et al., 2015), multiple
61 stressors (Breitburg et al., 2015), and compensatory processes (Cross, Harper, & Peck, 2019;
62 Ghedini, Russell, & Connell, 2015; Leung, Russell, & Connell, 2017), as well as predictive
63 models which often exclude important biological mechanisms (Urban et al., 2016). Therefore, a
64 better mechanistic understanding of environmental sources and processes mediating species'
65 responses to disturbances is critical for building the theoretical baseline necessary to forecast the
66 combined effects of multiple emerging stressors (Kroeker et al., 2017; Urban et al., 2016).

67 Advances in macroecology suggest that permanent environmental mosaics, defined by spatial
68 overlaps of non-monotonic environmental gradients (Kroeker et al., 2016), as well as regional
69 adaption or acclimatisation (Calosi et al., 2017; Peck, 2018; Vargas et al., 2017), dictate
70 geographic variations in species performance and sensitivity to disturbances in marine
71 ecosystems. Key to these works is that responses vary among populations and taxa (Calosi et al.,
72 2017; Kroeker et al., 2013; Telesca et al., 2018), which often play disproportionately strong roles
73 in structuring benthic communities (Ashton, Morley, Barnes, Clark, & Peck, 2017). Thus,
74 species-specific biological processes driving organismal variability likely shape differential
75 regional responses of foundation species to co-occurring multiple drivers. This can establish

76 spatial patterns of unexpected susceptibility of marine communities to future environmental
77 conditions.

78 Species producing calcium carbonate (CaCO_3) shells and skeletons are possibly experiencing the
79 strongest impacts of rapid environmental changes (Kroeker et al., 2013). Knowledge of their
80 sensitivity is derived largely from short- to long-term studies on model organisms (Kroeker et
81 al., 2013; Nagelkerken & Connell, 2015), while complex variations under multiple stressors in
82 natural environments have rarely been investigated (Ashton et al., 2017; Kroeker et al., 2016;
83 Peck et al., 2015; Watson, Morley, & Peck, 2017). Therefore, inferences made from
84 experimental studies may not necessarily translate to complex marine ecosystems (Connell et al.,
85 2017; Vargas et al., 2017). Indeed, species-specific responses to habitat alterations (Kroeker et
86 al., 2013), on top of mixed outcomes of environmental interactions (Crain, Kroeker, & Halpern,
87 2008), make future ecosystem predictions extremely challenging (Kroeker et al., 2017). This
88 leaves open the question: do differences in biological processes, shaping regional variations of
89 calcifiers' responses to interacting environmental stressors, define geographic patterns of
90 unanticipated species sensitivity or resilience to global environmental change?

91 A body of research has focused on responses of marine calcifiers to altered water chemistry
92 (Kroeker et al., 2013; Nagelkerken & Connell, 2015), but studies have rarely considered changes
93 in biogeochemical cycles strongly mediating biological responses to disturbance (Gattuso et al.,
94 2015). Among those, a marked intensification of the global water cycle in response to warming
95 (+4% for +0.5 °C) has been documented over recent decades through changes in ocean salinity
96 (Durack, Wijffels, & Matear, 2012). Salinity is a major ecological factor dictating distribution
97 and survival of aquatic organisms, ecosystem functioning (Solan & Whiteley, 2016), as well as
98 conditions for biomineralisation (Thomsen, Haynert, Wegner, & Melzner, 2015). Indeed, salinity

99 correlates positively with the availability of calcification substrates [bicarbonate (HCO_3^-) and
100 calcium (Ca^{2+}) ion concentrations] and, therefore, seawater CaCO_3 saturation state (Ω_{CaCO_3})
101 (Thomsen, Ramesh, Sanders, Bleich, & Melzner, 2018). Saturation states of the two main CaCO_3
102 polymorphs [calcite (Ω_{calc}) and aragonite (Ω_{arag})] control calcification kinetics, driving net
103 deposition or dissolution of CaCO_3 structures (Ries, Ghazaleh, Connolly, Westfield, & Castillo,
104 2016; Sanders, Schmittmann, Nascimento-Schulze, & Melzner, 2018; Thomsen et al., 2018).
105 Multidecadal studies have revealed a global salinity pattern following the “rich-get-richer”
106 mechanism, where salty ocean regions (compared to the global mean) are getting saltier (mid-
107 latitudes), whereas low salinity regions are getting fresher (tropical convergence zones and polar
108 regions) (Durack et al., 2012). In a future 2 - 3 °C warmer world, a substantial 16 - 24%
109 intensification of the global water cycle is predicted to occur, making salinity gradients much
110 sharper (Durack et al., 2012). This may affect deposition rates of biogenic CaCO_3 through
111 altered calcification costs. However, the emergent ecological effects of changing salinity on
112 calcifying species are largely unknown.

113 Atlantic blue mussels, *Mytilus edulis* and *M. trossulus*, are important bed-forming foundation
114 species throughout the eulittoral ecosystems of the northern hemisphere, and represent valuable
115 resources for aquaculture (192,000 t produced in 2016 worth 325 million USD) (FAO, 2017).
116 Growing awareness of the consequences of climate change on biodiversity and the industry that
117 *Mytilus* species support has stimulated a number of studies to estimate their response potential to
118 changing ocean conditions (Telesca et al., 2018; Thomsen et al., 2017; Thyrring, Blicher,
119 Sørensen, Wegeberg, & Sejr, 2017).

120 Calcareous shells perform a range of vital functions including structural support and protection
121 against predators. Because shell integrity determines survival, shell traits are subject to strong

122 selection pressure with functional success or failure a fundamental evolutionary driver. Blue
123 mussel shell consists of three layers (Fig. 1a,b): (1) the outer organic periostracum, and the
124 calcified (2) anvil-type fibrous prismatic and (3) nacreous layers. The periostracum is made of
125 sclerotised (quinone-tanned) proteins. This layer provides a protected environment for the
126 deposition of calcareous components, and protects shells from corrosive, acidic waters as well as
127 predatory and endolithic borers (Harper, 1997). The fibrous prismatic and nacreous layers are
128 composed of CaCO₃ crystals of different mineral forms, calcite and aragonite respectively, and
129 inter-crystalline biomineral organic matrix (Checa, Pina, Osuna-Mascaró, Rodríguez-Navarro, &
130 Harper, 2014). These calcareous layers are characterised by different microstructures (Fig. S1)
131 and more (i.e. aragonite) or less (i.e. calcite and organics) soluble components (Harper, 2000;
132 Mucci, 1983), the combination of which determines specific chemical and mechanical shell
133 protection characteristics (Barthelat, Rim, & Espinosa, 2009; Currey & Taylor, 1974; Fitzer et
134 al., 2015). Differences in energetic costs of making shell components (Palmer, 1992; Watson et
135 al., 2017), combined with future alterations in environmental gradients (Gattuso et al., 2015) and
136 water carbonate chemistry (Thomsen, et al., 2015; Thomsen et al., 2018), will likely influence
137 variations in shell production and composition, shaping regional patterns of shell resilience to
138 abiotic and biotic alterations.

139 *Mytilus* spp. growth, biomineralisation and fitness are linked to multiple drivers, including water
140 temperature, salinity and food supply [chlorophyll-*a* (Chl-*a*) concentration] (Sanders et al., 2018;
141 Thomsen, Casties, Pansch, Körtzinger, & Melzner, 2013). As is the case for all, but in the
142 context of this study, in the North Atlantic and Arctic Oceans these key environmental factors
143 vary heterogeneously with latitude (Fig. 1c,d), encompassing a range of conditions predicted
144 under different future climate change scenarios (Kirtman et al., 2013). Here, we hypothesise that

145 plasticity in shell biomineralisation, driving spatial variations in shell production, mineral and
146 organic composition, i) shape regional responses of *Mytilus* species to interacting environmental
147 drivers, and ii) define geographic patterns of blue mussel vulnerability in the face of global
148 environmental changes.

149 Despite projected alterations of salinity (Durack et al., 2012; Gattuso et al., 2015) and, therefore,
150 water carbonate chemistry (Ω_{CaCO_3}) and calcification costs (Sanders et al., 2018; Thomsen et al.,
151 2018), salinity gradients have been overlooked in large-scale predictive models for marine
152 calcifiers. This knowledge is essential to forecast whether environmental changes affect shell
153 variability and functional capability, especially in ecologically important foundation species such
154 as *M. edulis* and *M. trossulus*. These factors are crucial for understanding species susceptibility
155 to other rapidly emergent stressors, such as warming, acidification, and altered species
156 interactions (Kroeker et al., 2017).

157 In this study, we examine the relationships between variations in *Mytilus* spp. shell
158 biomineralisation, from juveniles to large adults, and interactive environmental gradients of
159 temperature, salinity and Chl-*a* concentration in 17 populations spanning a latitudinal range of
160 30° (3,334 km) across the Atlantic-European and Arctic coastline (Fig. 1c,d). In particular, we
161 tested for a latitudinal effect on blue mussel shell calcification that we hypothesise will show a
162 general decrease from temperate to polar regions. We also identified environmental sources of
163 within-region variations in shell production and composition, to test whether salinity affects shell
164 biomineralisation during growth, suggesting changes of shell structure, mechanical and chemical
165 properties. Finally, we modelled spatial trends in shell deposition with environmental gradients,
166 to test whether plasticity in shell biomineralisation shapes regional responses of *Mytilus* species
167 to interacting stressors, defining geographic patterns of sensitivity to future changes.

168 **MATERIALS AND METHODS**

169 ***Mytilus* collection**

170 We sampled individuals from 17 *Mytilus* (*M. edulis* and *M. trossulus*) populations along the
171 North Atlantic, Arctic, and Baltic Sea coastlines from four distinctive climatic regions (warm-
172 temperate, cold-temperate, subpolar and polar) covering a latitudinal range of 30° (a distance of
173 3,334 km), from Western European (Brest, North-West France, 48°N) to Northern Greenlandic
174 (Qaanaaq, North-West Greenland 78°N) coastlines (Fig. 1c). During December 2014 -
175 September 2015, mussels of various size classes for each site (shell length 26 - 81 mm) were
176 sampled from the eulittoral zone on rocky shores for a total of 424 individuals (Table S1). At
177 each site, specimens were collected from the lower limit of the intertidal zone (0 - 0.5 m above
178 the zero tidal level) on rocky substratum to allow for comparisons (in terms of local conditions)
179 between Atlantic and Baltic mussels, the latter experiencing short and irregular periods of air
180 exposure during the year. For each specimen, shell length was measured with digital calipers
181 (0.01 mm precision) and used as a within-population (collection site) proxy for age (Seed &
182 Richardson, 1990).

183 We analysed *Mytilus* populations for which the genetic structure was known, with particular
184 focus on species identity and hybrid status (*M. edulis* × *M. trossulus*). Genetic studies have
185 revealed various episodes of extensive introgression of *M. edulis* alleles in *M. trossulus*
186 populations and pronounced hybridisation patterns, especially in the Baltic Sea (Riginos &
187 Cunningham, 2005; Stuckas, Stoof, Quesada, & Tiedemann, 2009), resulting in the absence of
188 “pure” *M. trossulus* populations at the North Atlantic and Baltic Sea scales. *Mytilus* shells used
189 were either from individuals already evaluated in genetic investigations or mussels obtained

190 from sites routinely used in regional monitoring programs that provided information on genetic
191 status (Table S1). Areas where the Mediterranean mussel, *Mytilus galloprovincialis*, was known
192 to be present were avoided. We did, however, sample a few sites (3) with very low levels of *M.*
193 *edulis* × *M. galloprovincialis* hybridisation. Here, mussels from the *M. edulis* species-complex
194 were analysed together because: i) they share the same shell microstructure (Fig. S1), ii) they
195 inhabit a wide range of similar habitats in the eulittoral zone, iii) their pervasive hybridisation
196 patterns (with differential introgression) excluding pure *M. trossulus* populations at the spatial
197 scale analysed, and iv) the documented smaller contribution of genetic status than environmental
198 heterogeneity on the variability of *Mytilus* shell traits across large geographic scales (Krapivka et
199 al., 2007; Telesca et al., 2018).

200

201 **Mussel shell preparation**

202 We set left shell valves in polyester resin (Kleer-Set FF, MetPrep, Coventry, U.K.) blocks.
203 Embedded specimens were sliced longitudinally along their axis of maximum growth (Fig. 1a)
204 using a diamond saw and then progressively polished with silicon carbide paper (grit size: P800 -
205 P2500) and diamond paste (grading: 9 - 1 µm). Photographs of polished sections (Fig. 1b) were
206 acquired with a stereo-microscope (Leica M165 C equipped with a Leica DFC295 HD camera,
207 Leica, Wetzlar, Germany) and shell thickness was measured using the Fiji software (v1.51w).
208 Since larger individuals had undergone evident environmental abrasion or dissolution which
209 removed the periostracum and prismatic layer closer to the umbo, we estimated the thickness of
210 the whole-shell, prismatic and nacreous layers at the midpoint along the shell cross-section.
211 Periostracum thickness was measured at the posterior edge where it attaches to the external side

212 of the prismatic layer, to estimate the fully formed organic layer that was unaffected by decay or
213 abrasion (Harper, 1997).

214

215 **Organic content analyses**

216 We performed thermogravimetric analyses (TGA) to estimate the weight proportion (wt%) of
217 organic matrix within the prismatic layer. A random subsample of 20 *Mytilus edulis* specimens
218 were selected from four populations (sites 1, 11, 15, 16) to explore differences in shell organic
219 content under temperate and polar regimes. We removed the periostracum by sanding, and tiles
220 of prismatic layer (8×5 mm, $n = 20 \times 4$ sites) were cut along the posteroventral shell margin.
221 Tiles were cleaned, air-dried and then finely ground. We tested ten milligrams of this powdered
222 shell with a thermogravimetric analyser (TGA Q500, TA Instruments, New Castle, DE, U.S.A.).
223 Samples were subjected to constant heating from ~ 25 °C to 700 °C at a linear rate of 10 °C min^{-1}
224 under a dynamic nitrogen atmosphere and weight changes were recorded (Supporting Document
225 S1). We estimated the wt% of organic matter within the shell microstructure as the proportion of
226 weight loss during the thermal treatment between 150 °C and 550 °C (Fig. S2). The TGA
227 method was used in preference to the traditional muffle furnace approach to explore changes in
228 organic matrix within a specific shell layer (intra- and inter-crystalline organics). Although
229 traditional approaches are still used to measure variation of organic content at the whole-shell
230 level (i.e. estimates of total organics including organic matrix, shell ligament and organics-rich
231 layers, such as the periostracum and myostracum) (Sanders et al., 2018), TGA represents a more
232 accurate and widely used method to provide an unbiased estimate (i.e. no influence of residual
233 intracrystalline water) of the wt% of organic matrix at a single microstructure level in molluscs

234 (Checa, Macías-Sánchez, Harper, & Cartwright, 2016; Zaremba, Morse, Mann, Hansma, &
235 Stucky, 1998). In a cross calibration experiment where samples of blue mussel shells were
236 analysed both in a muffle furnace and by TGA ($n = 5 \times 4$ sites), results obtained were not
237 significantly different (Fig. S3).

238

239 **Environmental characterisation**

240 We selected three key environmental drivers based on their known influence on mussel growth
241 and calcification, their level of collinearity across the geographic scale investigated, and the
242 forecasted major ocean alterations under climate change (Kirtman et al., 2013; Sanders et al.,
243 2018; Thomsen, et al., 2013). For each site measurements of sea surface temperature, salinity,
244 and Chl-*a* concentration, the latter being used as a proxy for food supply (Thomsen, et al., 2013),
245 were generated using the Copernicus Marine Environment Monitoring Service (CMEMS)
246 (<http://marine.copernicus.eu/>). These climate datasets are composed of high-resolution physical
247 and biogeochemical assimilated (iterative integration of new observational information and
248 model forecasts over time) daily data (Supporting Document S2). To provide a first order mean
249 approximation of the average water conditions prevailing during the periods of mussel growth
250 and shell deposition (Carter & Seed, 1998; Thomsen, et al., 2010) across the life-span of both
251 young and adult sampled specimens from different age classes (between two and six years old),
252 we expressed parameters as mean May - October values averaged over the 6-year period 2009 -
253 2014 (daily observation, $n = 2,191$ per parameter) and used these as input variables (Fig. 1d;
254 Table S2).

255 Direct environmental monitoring for each site was not feasible due to the number and geographic
256 range (> 3,300 km latitudinal span) of the mussel populations analysed, the absence of direct
257 records for many of the sites used, and the temporal resolution (daily data over six years)
258 required to provide an average estimate for the growth conditions of young and adult specimens.
259 For this large-scale study, assimilated data presented potential advantages compared to
260 traditional measurements due to their spatial and temporal extent, repetition over time, advanced
261 calibration and validation (i.e. high correlation with discrete field measurements) (IOCCG, 2014;
262 Telesca et al., 2018; Thomas et al., 2011).

263

264 **Statistical analysis**

265 Generalised linear (mixed) models, GL(M)Ms, were used to explain shell thickness and
266 composition, from juveniles to large adults, with respect to latitude and environmental drivers,
267 and to compare between the individual shell layers. GLMMs were applied i) to account for the
268 hierarchical structure of the dataset consisting of multiple specimens ($n = 24 - 26$ replicates)
269 from each collection site, ii) to control for variations (“noise”) among sampling units (collections
270 sites) due to local habitats, and iii) to generalise our results to Atlantic *Mytilus* populations
271 beyond the study sample (Bolker, 2015; Zuur, Ieno, Walker, Saveliev, & Smith, 2009).

272 We carried out data exploration following the protocol of Zuur et al. (2010). Initial inspection
273 revealed no outliers. Pairwise scatterplots and variance inflation factors (VIFs) were calculated
274 to check for collinearity between input variables. VIF values < 2 indicated an acceptable degree
275 of correlation among covariates to be included within the same model. We applied residual
276 regression to uncouple the unique from the shared contribution of temperature and Chl-*a*

277 concentration to the response (Graham, 2003). This allowed us to account for the existing causal
278 link between these two parameters and to avoid inferential problems from modelling non-
279 independent covariates without losing explanatory power (Graham, 2003). To directly compare
280 model estimates (effect size metrics) from predictors on different measurement scales, to
281 estimate biologically meaningful intercepts, and to interpret main effects when interactions are
282 present, we standardised all the input variables (environmental parameters and shell length)
283 (Grueber, Nakagawa, Laws, & Jamieson, 2011; Schielzeth, 2010). For standardisation, we
284 subtracted the sample mean from the variable values and divided them by the sample standard
285 deviation [$z_i = (x_i - \bar{x})/\sigma_x$] (Schielzeth, 2010).

286 We used separate GLMMs to explore patterns of whole-shell and periostracum thickness with
287 latitude, environmental conditions, and shell length (size) ($n = 424$). A different approach was
288 used to investigate relationships between calcareous layers and latitudinal gradients. Prismatic
289 and nacreous layer thickness were analysed within the same GLMM ($n = 424 \times 2$ layers) to i)
290 estimate their variation and covariation across latitudes, ii) predict simultaneously common and
291 divergent environmental effects on both layers, and iii) reduce the probability of type I error. To
292 model the relationship between layer thickness and latitude we used a GLMM with a normal
293 distribution with latitude (continuous), shell layer (categorical, two levels: prismatic and
294 nacreous) and their interaction as fixed covariates. To model shell thickness as a function of the
295 environmental predictors we used a GLMM with a normal distribution (Equation 1). In the initial
296 model, fixed continuous covariates were standardised temperature, salinity and Chl-*a* in addition
297 to shell layer (categorical, two levels) and their two-way interactions. Shell length (continuous)
298 was included in both models to control for possible effects of within-population size variation on
299 layer thickness. To incorporate the dependency among observations for a specific layer from the

300 same collection site, we used site as a random intercept. Preliminary inspection of models'
301 residuals showed heteroscedasticity in most models. The use of different continuous probability
302 distributions (i.e. gamma and inverse Gaussian) and link functions did not stabilise the variance,
303 therefore a ln-transformation of the response was required. Response variables did not require
304 further transformations.

305 The proportion (wt%) of organic matrix in the prismatic layer ($n = 80$) was modelled with GLMs
306 as a function of collection site (categorical, four levels) and prismatic thickness (continuous) to
307 test for differences between polar and temperate regions and association with shell thickness.
308 The response variable was coded as a value from 0 to 1; therefore, we used a GLM with a beta
309 distribution and a logistic link function. Pair-wise contrasts with a standard Bonferroni correction
310 (alpha of 0.0125) were then used to test for differences in wt% among sites within and between
311 climatic regions.

312 Models were optimised by first selecting the random structure and then the optimal fixed
313 component. The principal tools for model comparison were the corrected Akaike Information
314 Criterion (AICc) and bootstrapped likelihood ratio tests. Random terms were selected on prior
315 knowledge of the dependency structure of the dataset. Visual inspection of residual patterns
316 indicated violation of homogeneity in most cases. This required the use of variance structures
317 (generalised least squares) allowing the residual spread to vary with respect to shell layer. The
318 fixed component was optimised by rejecting only non-significant interaction terms that
319 minimised the AICc value. For all model comparisons, variation of AICc between the optimal
320 (lowest AICc value) and competing models were greater than 8, and fixed-effect estimates were
321 nearly identical, indicating that competing models were very unlikely to be superior (Burnham &
322 Anderson, 2002). The proportion of variance explained by the models was quantified with

323 conditional or pseudo determination coefficients (cR^2 or $\text{pseudo}R^2$) (Nakagawa, Johnson, &
324 Schielzeth, 2017). We used variograms to assess the absence of spatial autocorrelation. Final
325 models were validated by inspection of standardised residual patterns to verify GLMM
326 assumptions of normality, homogeneity and independence. We used optimal models fitted on
327 standardised input variables (same measurement scale) to estimate the mean effect sizes of
328 environmental drivers on the response (Schielzeth, 2010). Ninety-five per cent confidence
329 intervals (95% CIs) for the regression parameters were generated using bias-corrected parametric
330 bootstrap methods (10,000 iterations). 95% CIs were used for statistical inference due to
331 estimation of approximated significance values (p -value) in mixed-modelling. If the confidence
332 intervals did not overlap zero, then the effect was considered significant. Conditional modes and
333 variances of the random effect were calculated for each GLMM to inspect differences in
334 collection site-level effect on the variation of individual layer thickness after accounting for the
335 effect of environmental covariates and shell size (fixed component). All data exploration and
336 statistical modelling were performed in R (v3.4.1) (for packages see Table S3).

337 A principal component analysis (PCA), with a singular value decomposition method, was
338 performed on shell traits (i.e. thickness of prismatic layer, nacreous layer, and periostracum) to
339 observe variations in shell composition among individuals from different climatic regions. The
340 PCA was used to create new independent variables, the principal components (PCs), resulting
341 from the linear combinations of shell traits (Table S4), and to observe how these changed
342 together among populations.

343

344 **RESULTS**

345 **Latitudinal patterns of shell deposition**

346 GLMMs indicated a general decrease of *Mytilus* whole-shell thickness with increasing latitude
347 (95% CI = -0.36 to -0.01, $cR^2 = 0.81$) (Fig. 2, S4). We detected a significant negative
348 relationship between the prismatic and nacreous layers thickness and latitude (95% CI = -0.258
349 to -0.068, $cR^2 = 0.71$; Fig. 2, S4), while no variation in periostracum thickness (95% CI = -0.14
350 to 0.07, $cR^2 = 0.81$; Fig. 2) was detected. No significant change in the relative thickness of
351 prismatic and nacreous layers was observed across the sampled latitudinal range (latitude \times layer
352 interaction, 95% CI = -0.24 to 0.15; Table S5). Shell length was positively correlated with
353 thickness in all layers indicating thickening during growth (Fig. 2; Table S5).

354 Prismatic layers were characterised by a significantly higher wt% of organic content (lower
355 proportion of $CaCO_3$) in mussel shells from polar than temperate regions, indicating decreased
356 shell calcification at high latitudes (Fig. 3a, S3). Polar shells [sites 15, 16; mean (SD) = 1.8 wt%
357 (0.31)] were characterised by an average of 29% more organic content compared to temperate
358 mussels [sites 1, 11; mean (SD) = 1.4 wt% (0.16)]. The wt% of organics was negatively
359 correlated with prismatic thickness (Fig. 3b), indicating a lower proportion of $CaCO_3$ and
360 thinner, less calcified, shells at polar latitudes.

361

362 **Environmental influence on shell production and composition**

363 We identified significant trends in shell thickness with environmental gradients depending on the
364 shell measurement considered (Fig. 2, S5; Table 1). Whole-shell thickness was positively related

365 to temperature, salinity and shell length, but there was no influence of Chl-*a* ($cR^2 = 0.93$; Fig. 2).
 366 Salinity had an effect on shell thickness that was 3.4 and 2.1 times larger than temperature and
 367 length, respectively (Fig. 2; Table 1).

368 Prismatic and nacreous layer thicknesses were analysed within the same GLMM. After model
 369 selection, fixed continuous covariates of the optimal model, Equation (1), were standardised
 370 *temperature*, *salinity*, *Chl-a*, *shell length* in addition to *shell layer* (categorical, two levels:
 371 prismatic and nacreous) and the *salinity* \times *layer*, *length* \times *layer* interactions. The random
 372 component was collection *site* used as a random intercept. The model was of the form:

$$373 \ln(Thickness_{ijk}) \sim N(\mu_{ijk}; \sigma_j^2)$$

$$374 \mu_{ijk} = Temperature_{ik} + Salinity_{ik} + Chl-a_{ik} + Length_{ik} + Layer_j$$

$$375 + Salinity_{ik} \times Layer_j + Length_{ik} \times Layer_j + Site_{ij}$$

$$376 Site_{ij} \sim N(0; \sigma_{Site}^2)$$

377 (Equation 1)

378 where $Thickness_{ijk}$ is the k th thickness observation from layer j ($j = \text{prismatic, nacreous}$) and site i
 379 ($i = 1, \dots, 17$). $Site_{ij}$ is the random intercept for layer j , which is assumed to be normally
 380 distributed with expectation 0 and variance σ_{Site}^2 .

381 Sea surface temperature, salinity and shell length all successfully predicted ($cR^2 = 0.93$)
 382 variations in the thickness of prismatic and nacreous layers, while no influence of Chl-*a* on either
 383 layer was detected (Table 1). The mean effect size of salinity on the response was twice as large
 384 as the effect of shell length, while it was 2.9 and 4.7 times larger than the effect of temperature
 385 on the prismatic and nacreous layers, respectively (Equation 2; Fig. 2). This indicates salinity

386 had a stronger contribution to predicting shell structure than the effects of temperature, Chl-*a*,
387 and shell length combined (Fig. 4).

388 $\mu_{ijk} =$

389
$$\begin{cases} 5.907 + 0.138 \times \text{Temperature} + 0.396 \times \text{Salinity} + 0.028 \times \text{Chl-}a + 0.197 \times \text{Length} & \text{Prismatic} \\ 5.853 + 0.138 \times \text{Temperature} + 0.654 \times \text{Salinity} + 0.028 \times \text{Chl-}a + 0.308 \times \text{Length} & \text{Nacreous} \end{cases}$$

390 (Equation 2)

391 Interactions between shell layer and both salinity and shell length (Equation 2) indicate
392 deposition of proportionally thicker prismatic layers (higher proportion of calcite) under low
393 salinities and proportionally thicker nacreous layers (higher proportion of aragonite) under
394 higher salinities across the entire range of shell lengths (Fig. 4). No change in the relative
395 thickness of prismatic and nacreous layers with water temperature was detected (Table S6).

396

397 **Periostracum variability**

398 Models of periostracum thickness revealed significant exponential relationships with Chl-*a* and
399 shell length ($cR^2 = 0.81$) (Table 1). Length had a mean effect that was three times larger than
400 Chl-*a* (Fig. 2), showing a rapid thickening of the periostracum during shell growth. The
401 interactions between shell length and both salinity and temperature indicate that the effects of
402 these variables on the periostracum were interdependent. At low salinities, the higher values of
403 shell length had a greater positive effect on periostracum thickness, while the reverse was true
404 for higher temperatures which had a marginal effect only on thickening rates (Fig. 5a, S6). This
405 suggests that periostracum thickening during shell growth was faster in fresher waters than in
406 relatively saltier conditions.

407

408 **Among-site shell variation**

409 GLMMs showed no difference in collection site-level effects (conditional modes) on each
410 thickness measurement (Fig. 5b). Conditional modes indicated that environmental factors and
411 shell size accounted for most of the among-site shell variations. This suggested no residual effect
412 of species identity or hybridisation (or other potentially influential factors) on the thickness of
413 individual shell layers at different sites after accounting for the effects of environmental
414 conditions and shell size.

415 A PCA on shell traits indicated marked differences in shell composition among sites from
416 different climatic regions (Fig. S7). PC1 captured most of the shell variation among individual
417 (74.7%) indicating differences in shell composition due to the wide range of size classes (shell
418 length) available. PC2 (16.9%) indicating formation of shells with thicker periostracum in low-
419 salinity environments (polar and Baltic region). PC3 (8.36%) captured heterogeneous within-
420 region variations in prismatic and nacreous layers deposition, supporting no change in the
421 relative deposition of calcareous shell components with latitude.

422

423 **DISCUSSION**

424 Our results demonstrate that plasticity in shell biomineralisation in *Mytilus* species shapes
425 regional differences in shell production and composition as a response to the spatial structure of
426 environmental conditions. An understanding of the biological processes driving differences in
427 responses of species among regions to multiple interacting stressors is crucial for improving

428 predictive accuracy and informing more realistic projections of species and ecosystem resilience
429 to climate change (Urban et al., 2016). Heterogeneous population-level responses from different
430 climates act as a natural laboratory for investigating potential effects of future change. These
431 differing responses suggest salinity is the best predictor of within-region variations in *Mytilus*
432 shell production, mineral (prismatic and nacreous layers) and organic (periostracum)
433 composition during growth. Spatial variations and trade-offs in shell biomineralisation suggest
434 geographic differences in chemical and mechanical protection, shaping spatial patterns of
435 resistance of these foundation species to global environmental changes.

436 Decreasing shell calcification (increasing organic content and thinner shells) towards high
437 latitudes (Fig. 2, 3) supports documented patterns of skeletal production and estimated costs
438 (Watson et al., 2017, 2012). Two explanatory paradigms exist for decreased skeletal size at
439 higher latitudes: i) increased calcification costs due to poleward decrease in Ω_{CaCO_3} and reduced
440 ectotherms metabolic rate (Watson et al., 2017, 2012) and ii) reduced predation pressure of
441 durophagous (shell crushing) and drilling predators (e.g. crabs, dog whelks and seabirds)
442 (Aronson et al., 2007; Harper & Peck, 2016). Given the higher production cost of shell organics
443 than CaCO_3 deposition (Palmer, 1992; Sanders et al., 2018; Watson et al., 2017) and problematic
444 protein production at polar temperatures (Peck, 2016, 2018), we might expect a reduced
445 proportion of organic matrix. Moreover, decreasing predation pressure should result in thinner
446 shells (Freeman, 2007; Sherker, Ellrich, & Scrosati, 2017) of the same composition irrespective
447 of geographic area. However, the wt% of organic matrix was higher at Arctic latitudes. This
448 could suggest either a marked increase in the cost of calcification in polar regions (Watson et al.,
449 2017), altering significantly the relative costs of organics and CaCO_3 production (Sanders et al.,
450 2018), or seawater Ω_{CaCO_3} below one ($\Omega \leq 1$) due to low temperatures and salinity

451 thermodynamically favouring net dissolution of CaCO₃ structures (Ries et al., 2016; Thomsen et
452 al., 2018). In either case, these effects would result in decreased shell calcification at high
453 latitudes. Increased proportions of insoluble organic matrix, which protects the calcified shell
454 components from dissolution (Harper, 2000), and deposition of thinner shells suggest a trade-off
455 between potential resilience to dissolving conditions and increased vulnerability to predators.
456 This may have adaptive beneficial effects on mussels in more corrosive, polar and subpolar
457 waters where predation pressure is low.

458 For over 60 years, temperature and shell size have been considered primary drivers of biogenic
459 CaCO₃ mineralogy across latitudes, dictating the formation of predominantly aragonitic
460 structures in temperate regions and increased calcite precipitation in cold climates (Carter &
461 Seed, 1998; Lowenstam, 1954; Ramajo, Rodriguez-Navarro, Duarte, Lardies, & Lagos, 2015).
462 Although our study partly corroborates previous findings, we observed no significant change in
463 the relative deposition of calcite (prismatic layer) and aragonite (nacreous layer) with latitude or
464 temperature. But we demonstrate that salinity had the strongest effect on shell production and
465 composition in Atlantic *Mytilus* (Fig. 2), supporting the strong influence of salinity on water
466 carbonate chemistry (Ω_{CaCO_3}) and calcification costs (Sanders et al., 2018; Thomsen, et al., 2015;
467 Thomsen et al., 2018).

468 The interaction between shell layer, salinity and shell size (Equation 2) indicates changes in shell
469 production (quantity) and composition (quality) in *Mytilus* spp. across different salinities (Fig.
470 4). Shifts in shell structure from juveniles to large adults lead to the formation of thinner,
471 prismatic-dominated shells in brackish waters and thicker, nacre-dominated structures under
472 marine conditions (Fig. 4b,c). Observed variations in predominant shell mineralogy with salinity
473 regime, suggest changes most likely driven by altered seawater carbonate saturation state. Low

474 temperatures and salinities in polar and subpolar regions, relative to temperate areas, would lead
475 to lower Ω_{CaCO_3} and favour net dissolution of the less stable of the two main forms of CaCO_3 ,
476 the aragonite (Mucci, 1983; Ries et al., 2016; Thomsen, et al., 2015), with formation of thinner,
477 calcite-dominated shells. Conversely, in temperate Atlantic regions, warmer and saltier waters
478 (higher Ω_{CaCO_3}) are less likely to constrain CaCO_3 production and deposition of thicker shells.
479 Very low salinities in the Baltic Sea, compared to the mean oceanic salinity, correlate with
480 limiting concentrations of calcification substrates (Thomsen et al., 2018) and lead to extended
481 period of aragonite undersaturation ($\Omega_{\text{arag}} < 1$), imposing kinetic constraints on calcification
482 (Tyrrell, Schneider, Charalampopoulou, & Riebesell, 2008). This will likely increase energetic
483 costs of calcification (Sanders et al., 2018; Thomsen et al., 2018) and favour net dissolution of
484 aragonite over calcite structures with formation of thinner shells characterised by higher
485 proportions of calcite (Melzner et al., 2011). No difference in site-level effects on individual
486 layers was found, suggesting modelled shell variations are independent of species identity and
487 hybridisation (Fig. 5b). This supports the relatively smaller contribution of genetic status than
488 environmental heterogeneity on the variability of *Mytilus* shell traits across large-geographic
489 scales suggested by Krapivka et al. (2007) and Telesca et al. (2018). Observed response patterns
490 suggest a strong potential for qualitative and quantitative shell adjustments in blue mussels to
491 produce the most appropriate shell structure for specific environmental conditions.

492 Under current scenarios, plasticity in shell biomineralisation could represent an advantageous
493 compensatory mechanism for *Mytilus* species when facing different water chemistries and
494 predation levels. In fact, at high-latitudes and in the Baltic region, where durophagous predators
495 are rare or absent (Aronson et al., 2007; Harper & Peck, 2016; Kautsky, Johannesson, &
496 Tedengren, 1990; Reimer & Harms-Ringdahl, 2001) and the water is more likely to constrain

497 CaCO₃ deposition ($\Omega_{\text{CaCO}_3} \leq 1$) (Watson et al., 2017), mussels are characterised by thinner,
498 prismatic-dominated (calcitic) shells enriched in organic matrix, providing a generally higher
499 protection from dissolution (Harper, 2000; Mucci, 1983). Conversely, at mid-latitudes, where
500 durophagous predators are more abundant (Harper & Peck, 2016; MacArthur, 1972) and
501 Ω_{CaCO_3} is generally higher (Watson et al., 2017), mussels display thicker, nacre-dominated
502 (aragonitic) shells suggesting higher mechanical resistance to predation (Barthelat et al., 2009;
503 Lowen, Innes, & Thompson, 2013; Sherker et al., 2017).

504 Despite projected global changes in salinity gradients (Durack et al., 2012), *Mytilus* species show
505 a strong capacity for compensatory responses in shell production to mitigate the emergent
506 negative effects of changing water chemistry. In fact, the interacting effects of salinity, shell
507 length, and a minor influence of temperature on the periostracum (Fig. 5a, S6), which represents
508 a strong chemical barrier to shell dissolution in molluscs (Harper, 1997; Peck, Tarling, Manno,
509 Harper, & Tynan, 2016; Tunnicliffe et al., 2009), indicated deposition of thicker periostraca
510 under decreasing salinities. This likely increases the durability of periostracum to environmental
511 abrasion during aging and better mediates impacts of ocean acidification.

512 Although populations in high-latitude ecosystems will experience globally the most rapid
513 acidification (Gattuso et al., 2015), decreasing salinity (lower Ω_{CaCO_3}) predicts deposition of
514 thinner shells with an increased proportion of organic-enriched, prismatic layers and thicker
515 periostraca, potentially increasing shell resistance to future more corrosive conditions.

516 Conversely, in temperate areas, increasing salinity (higher Ω_{CaCO_3}) predicts deposition of thicker
517 shells with relatively thicker nacreous layers, favouring mechanical protection from higher
518 predation pressure in warmer climates (Freeman, 2007; Harper & Peck, 2016; Lowen et al.,

519 2013; Sherker et al., 2017). However, forecasted changes in the thickness of periostracum with
520 salinity depend on shell size and would be more evident in larger or faster growing individuals
521 (length > 48 mm) (Fig. 5a).

522 In Greenland, where the rate of melting of the ice sheet has doubled in the last decade (Kjeldsen
523 et al., 2015), lower salinities during summer (< 20 psu) (Sejr et al., 2017), decreasing Ω_{CaCO_3} and
524 increasing primary productivity (food supply) in coastal areas (Meire et al., 2017), predict
525 formation of thicker periostraca and proportionally thicker organic-enriched calcitic layers.
526 These shell adjustments in Arctic *Mytilus* spp. could represent compensatory responses for a
527 potentially increased resilience to future water conditions favouring shell dissolution at the price
528 of decreased protection from predators. In contrast, in the Baltic Sea, the projected decrease in
529 salinity (up to 45% reduction in the north-eastern and central Baltic) (Gräwe, Friedland, &
530 Burchard, 2013), combined with the considerable physiological osmotic stress (salinity from 22
531 psu to 3 psu), would be particularly critical for mussels inhabiting already unfavourable
532 conditions for calcification (i.e. limiting $[\text{Ca}^{2+}]$ and aragonite undersaturated seawater) (Sanders
533 et al., 2018; Thomsen et al., 2018). Moreover, the reduced shell size of Baltic *Mytilus* does not
534 predict formation of thicker, durable periostraca, which could further increase vulnerability to
535 dissolution. Impacts of changing salinity on *Mytilus*, which contributes up to 90% of the Baltic
536 benthic invertebrate biomass (Kautsky et al., 1990), could have large-scale implications for
537 coastal communities in the near future (Johannesson, Smolarz, Grahn, & André, 2011).

538 *Mytilus* species have a marked shell plasticity and thick periostracum compared to other
539 calcifiers that often compete with it for space (e.g. barnacles and spirorbid polychaetes).
540 Biomineralisation plasticity may act as a mechanism conferring *Mytilus* species a protective
541 capacity for quantitative and qualitative trade-offs in shell deposition to produce the most

542 appropriate shell structure for a specific set of abiotic (i.e. CaCO₃ water chemistry and sources)
543 and biotic (i.e. predation pressure) conditions. This potential mechanism could represent a major
544 factor for keystone calcifiers, not only molluscs, to maintain their ecological role and functions
545 in rapidly changing oceans. Moreover, the periostracum provides a strong defence against shell
546 dissolution and allows mytilids to survive in oligohaline waters (~5 psu) and extremely acidified
547 conditions (e.g. hydrothermal vents) (Harper, 1997; Tunnicliffe et al., 2009). These factors may
548 shift the ecological balance and community structure in favour of species with a greater response
549 potential and stronger resistance to corrosive conditions, such as mussels, when ocean waters
550 become fresher and more acidic in future decades.

551 As hypothesised, plasticity in shell biomineralisation shapes regional differences in *Mytilus* shell
552 responses to interacting environmental conditions and drives spatial variations of chemical and
553 mechanical shell protection, dictating geographic patterns of Atlantic *Mytilus* sensitivity to future
554 environmental change. Overall, mussel shell calcification decreased towards high latitudes, with
555 salinity being the best predictor of within-region variations in shell production, mineral and
556 organic composition. Quantitative and qualitative differences in shell deposition among regions
557 indicate compensatory trade-offs in shell components suggesting the potential for a higher
558 resistance against dissolution for mussels in polar, low-salinity environments, and an enhanced
559 mechanical protection from predators in temperate, higher-salinity regions. The strong response
560 potential of blue mussel shell periostracum suggests a potentially increased resilience to ocean
561 acidification in polar and sub-polar *Mytilus*, and a higher sensitivity of Baltic populations under
562 future environmental conditions.

563 Our findings indicates that a better understanding of key biological processes mediating species'
564 response to habitat alterations will be essential for identifying vulnerability and informing

565 conservation practices, especially for species having both high climate sensitivity and key
566 ecological roles in shaping marine communities. This knowledge underpins our ability to predict
567 accurately and reduce the damaging effect of climate change on future biodiversity under any
568 range of scenarios (Urban et al., 2016). Our study has important implications because it explores
569 the links between i) the mechanisms of biological variation, as biomineralisation plasticity, ii)
570 species' responses to the spatial co-occurrence of multiple environmental drivers, and iii)
571 potential regional differences in resilience of calcifying species to habitat change. This
572 understanding is of critical importance for making realistic projections of emergent ecological
573 effects of global environmental changes, such as altered salinity regimes, and to improve our
574 predictive accuracy for impacts on marine communities and ecosystems, and the services they
575 provide.

576

577 **ACKNOWLEDGMENTS**

578 We thank Iain Johnston (Scottish Oceans Institute, St. Andrews, UK), Sarah Dashfield
579 (Plymouth Marine Laboratory, Plymouth, UK), Dr Peter Thor (Norwegian Polar Institute,
580 Tromsø, Norway), Dr Alexander Ventura (University of Gothenburg, Kristineberg, Sweden),
581 Prof Joseph Hoffman (Bielefeld University, Bielefeld, Germany), Dr Henk van der Veer and
582 Rob Dekker (Royal Netherlands Institute for Sea Research, Texel, Netherlands) for help with
583 specimens collection. We also thank Prof. Michael Carpenter (University of Cambridge, UK) for
584 help with furnace analyses and the Statistics Clinic (University of Cambridge, UK) for statistical
585 advice. The work was funded by the European Union Seventh Framework Programme, Marie
586 Curie ITN CALcium in a CHanging Environment (CACHE), under grant agreement n° 605051.

587 JT acknowledges additional financial support from the Independent Research Fund Denmark,
588 DFF-International Post-doc Grant n° 7027-00060B.

589

590 **REFERENCES**

591 Aronson, R. B., Thatje, S., Clarke, A., Peck, L. S., Blake, D. B., Wilga, C. D., & Seibel, B. A.
592 (2007). Climate change and invasibility of the Antarctic benthos. *Annual Review of*
593 *Ecology, Evolution, and Systematics*, 38(1), 129–154.

594 Ashton, G. V., Morley, S. A., Barnes, D. K. A., Clark, M. S., & Peck, L. S. (2017). Warming by
595 1 °C drives species and assemblage level responses in Antarctica’s marine shallows.
596 *Current Biology*, 27(17), 2698-2705.e3.

597 Barthelat, F., Rim, J. E., & Espinosa, H. D. (2009). A review on the structure and mechanical
598 properties of mollusk shells – Perspectives on synthetic biomimetic materials. In B.
599 Bhushan & H. Fuchs (Eds.), *Applied Scanning Probe Methods XIII* (pp. 17–44). Berlin,
600 Heidelberg: Springer.

601 Bolker, B. M. (2015). Linear and generalized linear mixed models. In G. A. Fox, S. Negrete-
602 Yankelevich, & V. J. Sosa (Eds.), *Ecological Statistics* (pp. 309–333). Oxford, UK: Oxford
603 University Press.

604 Breitburg, D. L., Salisbury, J., Bernhard, J., Cai, W.-J., Dupont, S., Doney, S., ... Tarrant, A.
605 (2015). And on top of all that... Coping with ocean acidification in the midst of many
606 stressors. *Oceanography*, 28(2), 48–61.

607 Burnham, K. P., & Anderson, D. R. (2002). *Model Selection and Multimodel Inference : a*
608 *Practical Information-Theoretic Approach*. New York, NY, USA: Springer-Verlag.

609 Calosi, P., Melatunan, S., Turner, L. M., Artioli, Y., Davidson, R. L., Byrne, J. J., ... Rundle, S.
610 D. (2017). Regional adaptation defines sensitivity to future ocean acidification. *Nature*
611 *Communications*, 8, 13994.

612 Carter, J. G., & Seed, R. (1998). Thermal potentiation and mineralogical evolution in *Mytilus*
613 (Mollusca; Bivalvia). In P. A. Johnston & J. W. Haggart (Eds.), *Bivalves: an Eon of*
614 *Evolution* (pp. 87–117). Vancouver: University of Calgary Press.

615 Checa, A. G., Macías-Sánchez, E., Harper, E. M., & Cartwright, J. H. E. (2016). Organic
616 membranes determine the pattern of the columnar prismatic layer of mollusc shells.
617 *Proceedings of the Royal Society B*, 283(1830), 20160032.

618 Checa, A. G., Pina, C. M., Osuna-Mascaró, A. J., Rodríguez-Navarro, A. B., & Harper, E. M.
619 (2014). Crystalline organization of the fibrous prismatic calcitic layer of the Mediterranean
620 mussel *Mytilus galloprovincialis*. *European Journal of Mineralogy*, 26(4), 495–505.

621 Connell, S. D., Doubleday, Z. A., Hamlyn, S. B., Foster, N. R., Harley, C. D. G., Helmuth, B., ...
622 Russell, B. D. (2017). How ocean acidification can benefit calcifiers. *Current Biology*,
623 27(3), R95–R96.

624 Crain, C. M., Kroeker, K., & Halpern, B. S. (2008). Interactive and cumulative effects of
625 multiple human stressors in marine systems. *Ecology Letters*, 11(12), 1304–1315.

626 Cross, E. L., Harper, E. M., & Peck, L. S. (2019). Thicker shells compensate extensive

627 dissolution in brachiopods under future ocean scidification. *Environmental Science &*
628 *Technology*, 53(9), 5016–5026.

629 Currey, J. D., & Taylor, J. D. (1974). The mechanical behaviour of some molluscan hard tissues.
630 *Journal of Zoology*, 173(3), 395–406.

631 Durack, P. J., Wijffels, S. E., & Matear, R. J. (2012). Ocean salinities reveal strong global water
632 cycle intensification during 1950 to 2000. *Science*, 336(6080), 455–458.

633 FAO. (2017). *FAO Yearbook. Fishery and Aquaculture Statistics. 2015*. Rome: FAO.

634 Fitzner, S. C., Zhu, W., Tanner, K. E., Phoenix, V. R., Kamenos, N. A., & Cusack, M. (2015).
635 Ocean acidification alters the material properties of *Mytilus edulis* shells. *Journal of the*
636 *Royal Society, Interface*, 12(103), 20141227.

637 Freeman, A. S. (2007). Specificity of induced defenses in *Mytilus edulis* and asymmetrical
638 predator deterrence. *Marine Ecology Progress Series*, 334, 145–153.

639 Gattuso, J. P., Magnan, A., Bille, R., Cheung, W. W. L., Howes, E. L., Joos, F., ... Turley, C.
640 (2015). Contrasting futures for ocean and society from different anthropogenic CO₂
641 emissions scenarios. *Science*, 349(6243), aac4722.

642 Ghedini, G., Russell, B. D., & Connell, S. D. (2015). Trophic compensation reinforces
643 resistance: herbivory absorbs the increasing effects of multiple disturbances. *Ecology*
644 *Letters*, 18(2), 182–187.

645 Graham, M. H. (2003). Confronting multicollinearity in ecological multiple regression. *Ecology*,
646 84(11), 2809–2815.

647 Gräwe, U., Friedland, R., & Burchard, H. (2013). The future of the western Baltic Sea: two
648 possible scenarios. *Ocean Dynamics*, 63(8), 901–921.

649 Grueber, C. E., Nakagawa, S., Laws, R. J., & Jamieson, I. G. (2011). Multimodel inference in
650 ecology and evolution: challenges and solutions. *Journal of Evolutionary Biology*, 24(4),
651 699–711.

652 Harper, E. M. (1997). The molluscan periostracum: an important constraint in bivalve evolution.
653 *Palaeontology*, 40(1), 71–97.

654 Harper, E. M. (2000). Are calcitic layers an effective adaptation against shell dissolution in the
655 Bivalvia? *Journal of Zoology*, 251(2), 179–186.

656 Harper, E. M., & Peck, L. S. (2016). Latitudinal and depth gradients in marine predation
657 pressure. *Global Ecology and Biogeography*, 25(6), 670–678.

658 IOCCG. (2014). *Phytoplankton Functional Types from Space. Reports of the International*
659 *Ocean-Colour Coordinating Group, No. 15.* (S. Sathyendranath, Ed.). Dartmouth: IOCCG.

660 Johannesson, K., Smolarz, K., Grahn, M., & André, C. (2011). The future of Baltic Sea
661 populations: Local extinction or evolutionary rescue? *AMBIO*, 40(2), 179–190.

662 Kautsky, N., Johannesson, K., & Tedengren, M. (1990). Genotypic and phenotypic differences
663 between Baltic and North Sea populations of *Mytilus edulis* evaluated through reciprocal
664 transplantations. I Growth and morphology. *Marine Ecology Progress Series*, 59, 203–210.

665 Kirtman, B., Power, S. B., Adedoyin, J. A., Boer, G. J., Bojariu, R., Camilloni, I., ... Wang, H. J.
666 (2013). Near-term climate change: projections and predictability. In T. F. Stocker, D. Qin,

667 G.-K. Plattner, M. Tignor, S. K. Allen, J. Boschung, ... P. M. Midgley (Eds.), *Climate*
668 *Change 2013: The Physical Science Basis. Contribution of Working Group I to the Fifth*
669 *Assessment Report of the Intergovernmental Panel on Climate Change* (pp. 953–1028).
670 Cambridge, UK: Cambridge University Press.

671 Kjeldsen, K. K., Korsgaard, N. J., Bjørk, A. A., Khan, S. A., Box, J. E., Funder, S., ... Kjær, K.
672 H. (2015). Spatial and temporal distribution of mass loss from the Greenland Ice Sheet since
673 AD 1900. *Nature*, 528(7582), 396–400.

674 Krapivka, S., Toro, J. E., Alcapán, A. C., Astorga, M., Presa, P., Pérez, M., & Guíñez, R. (2007).
675 Shell-shape variation along the latitudinal range of the Chilean blue mussel *Mytilus*
676 *chilensis* (Hupé 1854). *Aquaculture Research*, 38(16), 1770–1777.

677 Kroeker, K. J., Kordas, R. L., Crim, R., Hendriks, I. E., Ramajo, L., Singh, G. S., ... Gattuso, J.-
678 P. (2013). Impacts of ocean acidification on marine organisms: quantifying sensitivities and
679 interaction with warming. *Global Change Biology*, 19(6), 1884–1896.

680 Kroeker, K. J., Kordas, R. L., & Harley, C. D. G. (2017). Embracing interactions in ocean
681 acidification research: Confronting multiple stressor scenarios and context dependence.
682 *Biology Letters*, 13(3), 20160802.

683 Kroeker, K. J., Sanford, E., Rose, J. M., Blanchette, C. A., Chan, F., Chavez, F. P., ... Washburn,
684 L. (2016). Interacting environmental mosaics drive geographic variation in mussel
685 performance and predation vulnerability. *Ecology Letters*, 19(7), 771–779.

686 Leung, J. Y. S., Russell, B. D., & Connell, S. D. (2017). Mineralogical plasticity acts as a
687 compensatory mechanism to the impacts of ocean acidification. *Environmental Science &*

688 *Technology*, 51(5), 2652–2659.

689 Lowen, J., Innes, D., & Thompson, R. (2013). Predator-induced defenses differ between
690 sympatric *Mytilus edulis* and *M. trossulus*. *Marine Ecology Progress Series*, 475, 135–143.

691 Lowenstam, H. A. (1954). Factors affecting the aragonite:calcite ratios in carbonate-secreting
692 marine organisms. *The Journal of Geology*, 62(3), 284–322.

693 MacArthur, R. H. (1972). *Geographical Ecology : Patterns in the Distribution of Species*.
694 Princeton, NJ, USA: Princeton University Press.

695 Meire, L., Mortensen, J., Meire, P., Juul-Pedersen, T., Sejr, M. K., Rysgaard, S., ... Meysman, F.
696 J. R. (2017). Marine-terminating glaciers sustain high productivity in Greenland fjords.
697 *Global Change Biology*, 23(12), 5344–5357.

698 Melzner, F., Stange, P., Trübenbach, K., Thomsen, J., Casties, I., Panknin, U., ... Gutowska, M.
699 a. (2011). Food supply and seawater pCO₂ impact calcification and internal shell dissolution
700 in the blue mussel *Mytilus edulis*. *PLoS ONE*, 6(9), e24223.

701 Mucci, A. (1983). The solubility of calcite and aragonite in seawater at various salinities,
702 temperatures, and one atmosphere total pressure. *American Journal of Science*, 283(7),
703 780–799.

704 Nagelkerken, I., & Connell, S. D. (2015). Global alteration of ocean ecosystem functioning due
705 to increasing human CO₂ emissions. *Proceedings of the National Academy of Sciences of*
706 *the United States of America*, 112(43), 13272–13277.

707 Nakagawa, S., Johnson, P. C. D., & Schielzeth, H. (2017). The coefficient of determination R²

708 and intra-class correlation coefficient from generalized linear mixed-effects models
709 revisited and expanded. *Journal of The Royal Society Interface*, 14(134), 20170213.

710 Palmer, A. R. (1992). Calcification in marine molluscs: how costly is it? *Proceedings of the*
711 *National Academy of Sciences of the United States of America*, 89(4), 1379–1382.

712 Peck, L. S. (2016). A cold limit to adaptation in the sea. *Trends in Ecology & Evolution*, 31(1),
713 13–26.

714 Peck, L. S. (2018). Antarctic marine biodiversity: adaptations, environments and responses to
715 change. In S. J. Hawkins, A. J. Evans, A. C. Dal, L. B. Firth, & I. P. Smith (Eds.),
716 *Oceanography and Marine Biology: an Annual Review* (Vol. 56, p. 510). CRC Press.

717 Peck, L. S., Clark, M. S., Power, D., Reis, J., Batista, F. M., & Harper, E. M. (2015).
718 Acidification effects on biofouling communities: winners and losers. *Global Change*
719 *Biology*, 21(5), 1907–1913.

720 Peck, V. L., Tarling, G. A., Manno, C., Harper, E. M., & Tynan, E. (2016). Outer organic layer
721 and internal repair mechanism protects pteropod *Limacina helicina* from ocean
722 acidification. *Deep Sea Research Part II: Topical Studies in Oceanography*, 127, 41–52.

723 Ramajo, L., Rodriguez-Navarro, A. B., Duarte, C. M., Lardies, M. A., & Lagos, N. A. (2015).
724 Shifts in shell mineralogy and metabolism of *Concholepas concholepas* juveniles along the
725 Chilean coast. *Marine and Freshwater Research*, 66(12), 1147–1157.

726 Reimer, O., & Harms-Ringdahl, S. (2001). Predator-inducible changes in blue mussels from the
727 predator-free Baltic Sea. *Marine Biology*, 139(5), 959–965.

- 728 Ries, J. B., Ghazaleh, M. N., Connolly, B., Westfield, I., & Castillo, K. D. (2016). Impacts of
729 seawater saturation state ($\Omega_A = 0.4\text{--}4.6$) and temperature (10, 25 °C) on the dissolution
730 kinetics of whole-shell biogenic carbonates. *Geochimica et Cosmochimica Acta*, *192*, 318–
731 337.
- 732 Riginos, C., & Cunningham, C. W. (2005). Local adaptation and species segregation in two
733 mussel (*Mytilus edulis* × *Mytilus trossulus*) hybrid zones. *Molecular Ecology*, *14*(2), 381–
734 400.
- 735 Sanders, T., Schmittmann, L., Nascimento-Schulze, J. C., & Melzner, F. (2018). High
736 calcification costs limit mussel growth at low salinity. *Frontiers in Marine Science*, *5*, 352.
- 737 Schielzeth, H. (2010). Simple means to improve the interpretability of regression coefficients.
738 *Methods in Ecology and Evolution*, *1*(2), 103–113.
- 739 Seed, R., & Richardson, C. A. (1990). *Mytilus* growth and its environmental responsiveness. In
740 G. B. Stefano (Ed.), *The Neurobiology of Mytilus edulis* (pp. 1–37). Manchester, UK:
741 Manchester University Press.
- 742 Sejr, M. K., Stedmon, C. A., Bendtsen, J., Abermann, J., Juul-Pedersen, T., Mortensen, J., &
743 Rysgaard, S. (2017). Evidence of local and regional freshening of Northeast Greenland
744 coastal waters. *Scientific Reports*, *7*(1), 13183.
- 745 Sherker, Z., Ellrich, J., & Scrosati, R. (2017). Predator-induced shell plasticity in mussels hinders
746 predation by drilling snails. *Marine Ecology Progress Series*, *573*, 167–175.
- 747 Solan, M., & Whiteley, N. (2016). *Stressors in the Marine Environment*. Oxford, UK: Oxford

- 748 University Press.
- 749 Stuckas, H., Stoof, K., Quesada, H., & Tiedemann, R. (2009). Evolutionary implications of
750 discordant clines across the Baltic *Mytilus* hybrid zone (*Mytilus edulis* and *Mytilus*
751 *trossulus*). *Heredity*, *103*(2), 146–156.
- 752 Telesca, L., Michalek, K., Sanders, T., Peck, L. S., Thyrring, J., & Harper, E. M. (2018). Blue
753 mussel shell shape plasticity and natural environments: a quantitative approach. *Scientific*
754 *Reports*, *8*(1), 2865.
- 755 Thomas, Y., Mazurié, J., Alunno-Bruscia, M., Bacher, C., Bouget, J.-F., Gohin, F., ... Struski, C.
756 (2011). Modelling spatio-temporal variability of *Mytilus edulis* (L.) growth by forcing a
757 dynamic energy budget model with satellite-derived environmental data. *Journal of Sea*
758 *Research*, *66*(4), 308–317.
- 759 Thomsen, J., Casties, I., Pansch, C., Körtzinger, A., & Melzner, F. (2013). Food availability
760 outweighs ocean acidification effects in juvenile *Mytilus edulis*: laboratory and field
761 experiments. *Global Change Biology*, *19*(4), 1017–1027.
- 762 Thomsen, J., Gutowska, M. A., Saphorster, J., Heinemann, A., Trubenbach, K., Fietzke, J., ...
763 Melzner, F. (2010). Calcifying invertebrates succeed in a naturally CO₂-rich coastal habitat
764 but are threatened by high levels of future acidification. *Biogeosciences*, *7*(11), 3879–3891.
- 765 Thomsen, J., Haynert, K., Wegner, K. M., & Melzner, F. (2015). Impact of seawater carbonate
766 chemistry on the calcification of marine bivalves. *Biogeosciences*, *12*(14), 4209–4220.
- 767 Thomsen, J., Ramesh, K., Sanders, T., Bleich, M., & Melzner, F. (2018). Calcification in a

768 marginal sea – influence of seawater [Ca²⁺] and carbonate chemistry on bivalve shell
769 formation. *Biogeosciences*, 15(5), 1469–1482.

770 Thomsen, J., Stapp, L. S., Haynert, K., Schade, H., Danelli, M., Lannig, G., ... Melzner, F.
771 (2017). Naturally acidified habitat selects for ocean acidification – tolerant mussels. *Science*
772 *Advances*, 3(4), e1602411.

773 Thyrring, J., Blicher, M., Sørensen, J., Wegeberg, S., & Sejr, M. (2017). Rising air temperatures
774 will increase intertidal mussel abundance in the Arctic. *Marine Ecology Progress Series*,
775 584, 91–104.

776 Tunnicliffe, V., Davies, K. T. A., Butterfield, D. A., Embley, R. W., Rose, J. M., & Chadwick Jr,
777 W. W. (2009). Survival of mussels in extremely acidic waters on a submarine volcano.
778 *Nature Geoscience*, 2(5), 344–348.

779 Tyrrell, T., Schneider, B., Charalampopoulou, A., & Riebesell, U. (2008). Coccolithophores and
780 calcite saturation state in the Baltic and Black Seas. *Biogeosciences*, 5(2), 485–494.

781 Urban, M. C., Bocedi, G., Hendry, A. P., Mihoub, J.-B., Peer, G., Singer, A., ... Travis, J. M. J.
782 (2016). Improving the forecast for biodiversity under climate change. *Science*, 353(6304),
783 aad8466.

784 Vargas, C. A., Lagos, N. A., Lardies, M. A., Duarte, C., Manríquez, P. H., Aguilera, V. M., ...
785 Dupont, S. (2017). Species-specific responses to ocean acidification should account for
786 local adaptation and adaptive plasticity. *Nature Ecology & Evolution*, 1(4), 0084.

787 Watson, S.-A., Morley, S. A., & Peck, L. S. (2017). Latitudinal trends in shell production cost

788 from the tropics to the poles. *Science Advances*, 3(9), e1701362.

789 Watson, S.-A., Peck, L. S., Tyler, P. A., Southgate, P. C., Tan, K. S., Day, R. W., & Morley, S.
790 A. (2012). Marine invertebrate skeleton size varies with latitude, temperature and carbonate
791 saturation: implications for global change and ocean acidification. *Global Change Biology*,
792 18(10), 3026–3038.

793 Zaremba, C. M., Morse, D. E., Mann, S., Hansma, P. K., & Stucky, G. D. (1998).
794 Aragonite–hydroxyapatite conversion in gastropod (Abalone) nacre. *Chemistry of*
795 *Materials*, 10(12), 3813–3824.

796 Zuur, A. F., Ieno, E. N., & Elphick, C. S. (2010). A protocol for data exploration to avoid
797 common statistical problems. *Methods in Ecology and Evolution*, 1(1), 3–14.

798 Zuur, A. F., Ieno, E. N., Walker, N., Saveliev, A. A., & Smith, G. M. (2009). *Mixed Effects*
799 *Models and Extensions in Ecology with R*. New York, NY: Springer New York.

800

801 **TABLES**802 **Table 1. Environmental GLMMs summary.**

803 Estimated statistics and bootstrapped 95% CIs for regression parameters are reported for the
 804 modelled relationships between thickness of the various shell layers and whole-shell against
 805 standardised covariates. For the summary of model in Equation (1), estimates for group means,
 806 slopes, and standard errors are reported separately for the prismatic and nacreous layers (Table
 807 S6). (Parameters' significance is determined when the 95% CI does not include zero).

	Estimate	SE	95% CI	<i>t</i> -value	<i>p</i> -value (approximate)
Whole-shell*					
(Intercept)	6.617	0.051	6.517; 6.717	128.71	< 0.0001
Temperature	0.156	0.054	0.014; 0.240	2.89	0.013
Salinity	0.525	0.060	0.411; 0.672	8.69	< 0.0001
Chl- <i>a</i>	0.074	0.054	-0.042; 0.216	1.37	0.20
Length	0.248	0.037	0.181; 0.327	6.44	< 0.0001
Prismatic (Pr) & nacreous (Na)†					
(Intercept)Layer(Pr)	5.907	0.031	5.775; 6.038	188.31	< 0.0001
(Intercept)Layer(Na)	5.853	0.083	5.715; 5.990	70.81	< 0.0001
Temperature	0.138	0.033	0.016; 0.263	4.17	0.0008
Chl- <i>a</i>	0.028	0.033	-0.084; 0.141	0.86	0.40
Salinity × Layer(Pr)	0.396	0.039	0.262; 0.529	10.22	< 0.0001
Salinity × Layer(Na)	0.654	0.093	0.501; 0.811	7.07	< 0.0001
Length × Layer(Pr)	0.197	0.031	0.094; 0.295	6.39	< 0.0001
Length × Layer(Na)	0.308	0.065	0.196; 0.419	4.74	< 0.0001
Periostracum‡					
(Intercept)	3.500	0.048	3.406; 3.596	71.03	< 0.0001
Temperature	0.049	0.043	-0.036; 0.134	1.12	0.28
Salinity	-0.009	0.061	-0.131; 0.111	-0.14	0.89

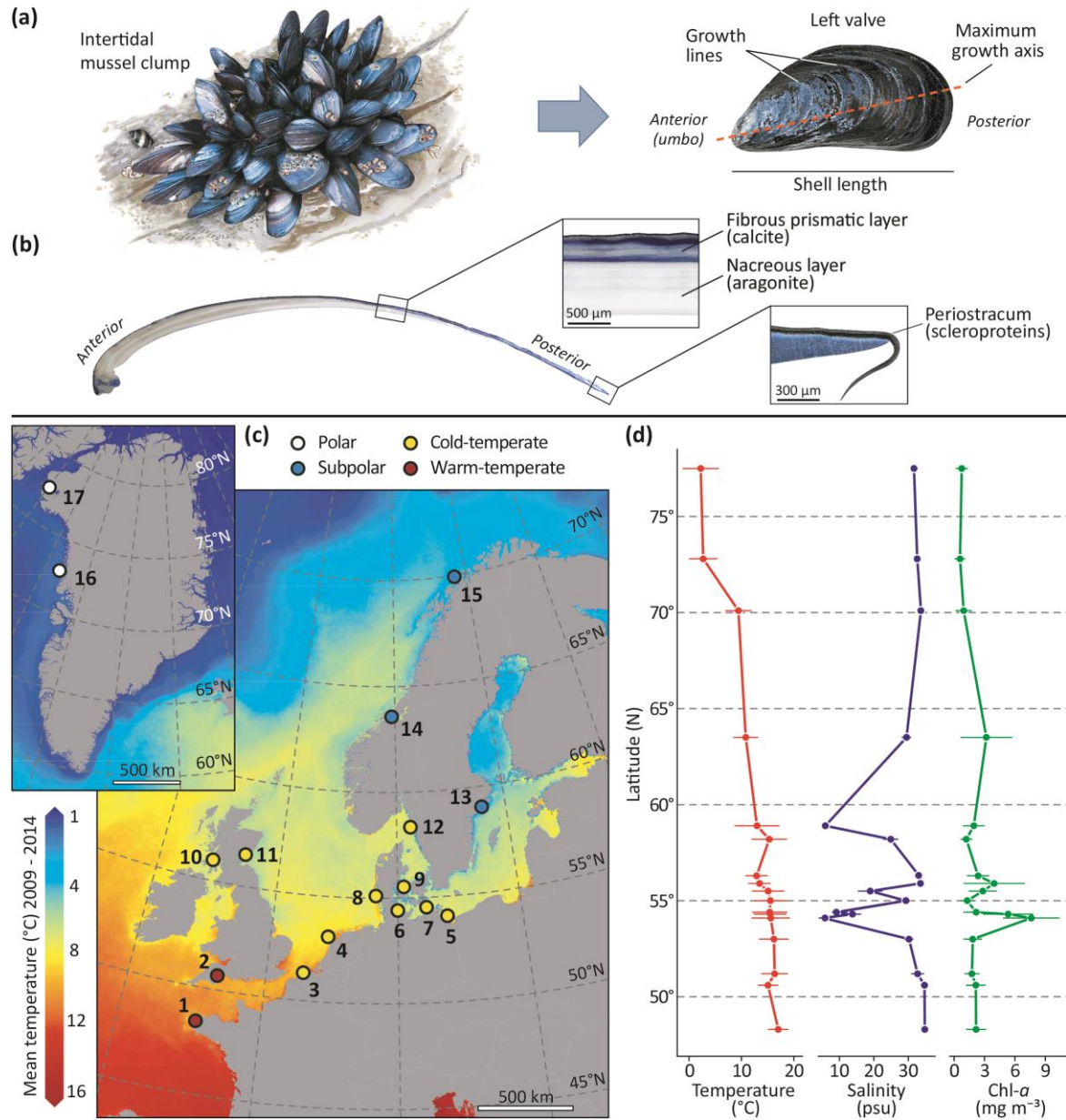
Chl- <i>a</i>	0.147	0.038	0.071; 0.221	3.88	0.0020
Length	0.439	0.041	0.357; 0.522	10.25	<0.0001
Temperature × Length	-0.064	0.035	-0.135; 0.006	-1.77	0.082
Salinity × Length	-0.151	0.061	-0.271; -0.029	-2.38	0.020

808 * Whole-shell, the random intercept was normally distributed with mean of 0 and variance
809 0.209².

810 † Prismatic and nacreous layers, the random intercepts were normally distributed with mean 0,
811 and variances 0.123² and 0.310², respectively.

812 ‡ Periostracum, the random intercept was normally distributed with mean 0 and variance 0.130².

813



815

816 **Figure 1.** *Mytilus* spp. shell, collection sites and environmental heterogeneity. **(a)** *Mytilus* shell

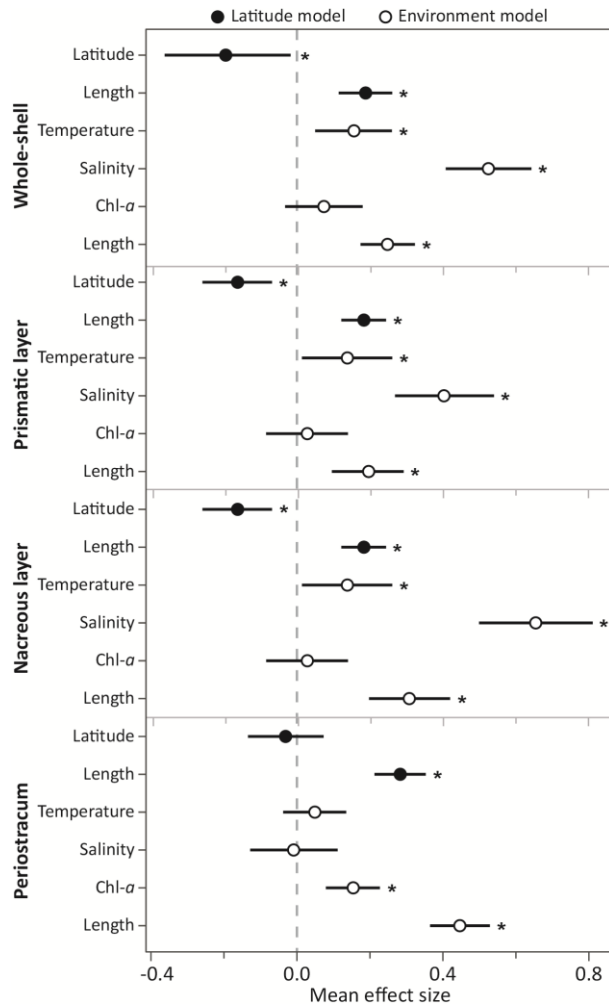
817 valve morphology and dimensions. **(b)** Anteroposterior cross-section of shell valve along the

818 axis of maximum growth (from umbo to posterior commissure, dashed line) showing internal

819 structure and composition of individual mineral (prismatic and nacreous) and organic

820 (periostracum) shell layers. **(c)** Thermal map of North-East Atlantic and Arctic surface waters

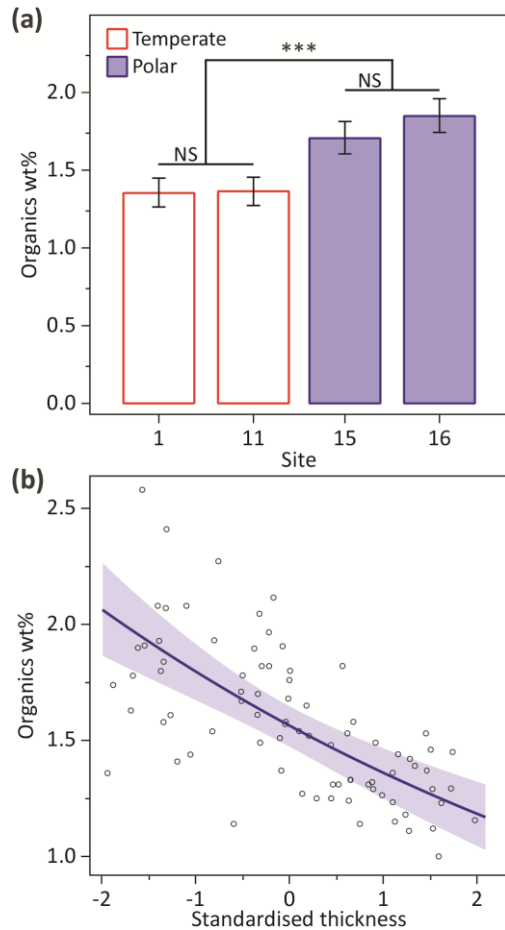
821 from the CMEMS (<http://marine.copernicus.eu/>) biogeochemical datasets showing locations at
822 different climatic regions (open circles) where *Mytilus* specimens were collected from across the
823 Eastern European and Greenlandic coastlines (from 48°N to 78°N): (1) Brest, France, (2)
824 Exmouth, England, (3) Oostende, Belgium, (4) Texel, Netherlands, (5) Usedom, (6) Kiel, (7)
825 Ahrenshoop, (8) Sylt, all Germany, (9) Kerteminde, Denmark, (10) Tarbet, Kintyre, Scotland,
826 (11) St. Andrews, Scotland, (12) Kristineberg, Sweden, (13) Nynäshamn, Sweden, (14)
827 Trondhiem, Norway, (15) Tromsø, Norway, (16) Upernavik, Greenland and (17) Qaanaaq,
828 Greenland. Map created with ArcMap 10.5 (ArcGIS software by Esri, <http://esri.com>),
829 background image courtesy of OpenStreetMap (<http://www.openstreetmap.org>). **(d)**
830 Heterogeneous latitudinal gradients for sea surface temperature, salinity, and Chl-*a* concentration
831 across the study regions. Mean values (May - October, filled circles) and SD (horizontal solid
832 lines) for the 6-year period 2009 - 2014 were estimated from CMEMS datasets.



833

834 **Figure 2.** Mean effect size of predictors on *Mytilus* shell measurements. Effect sizes were
 835 estimated from individual latitudinal (filled circles) and environmental (open circles) GLMMs.
 836 Mean effect sizes and direction of impacts of latitude, shell length, sea surface temperature,
 837 salinity, and Chl-*a* concentration on layer In-thickness (μm) measurements are reported for the
 838 whole-shell, prismatic layer, nacreous layer, and periostracum. Significance of regression
 839 parameters is identified when the bootstrapped 95% CI (error bars) does not cross zero (*
 840 denotes a significant difference from zero).

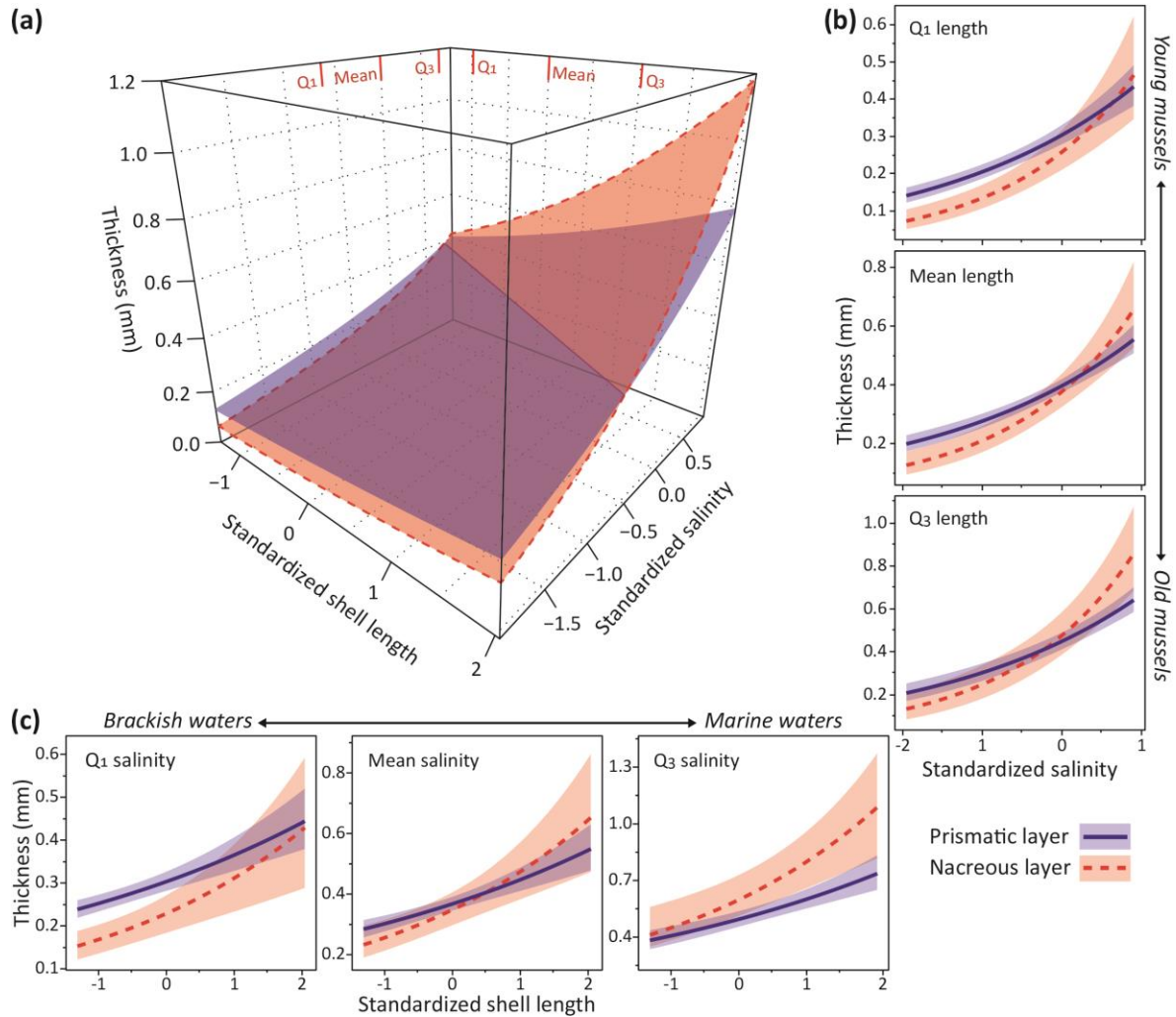
841



842

843 **Figure 3.** Latitudinal patterns of shell organic content and calcification. **(a)** Variations in organic
 844 content within prismatic layers among shells from temperate (sites 1, 11; open bars) and polar
 845 (sites 15, 16; solid bars) climates. Pair-wise contrasts indicated significantly higher proportions
 846 of organics in high-latitude than low-latitude specimens [mean difference = 0.44%; $z = 8.27$, $p <$
 847 0.0001 (***)], $\text{pseudo}R^2 = 0.49$, $n = 80$], in addition to non-significant differences (NS) among
 848 temperate (mean difference = 0.002%; $z = 0.12$, $p = 0.91$) and polar (mean difference = 0.13%, z
 849 $= 1.86$, $p = 0.063$) populations. Error bars indicate 95% CIs. **(b)** Relationship between the wt%
 850 of organics and standardised thickness of the prismatic [mean (SD) = 529 μm (174)] (sites 1, 7,
 851 10 and 11), indicating a negative association between layer thickness and calcification level ($z =$

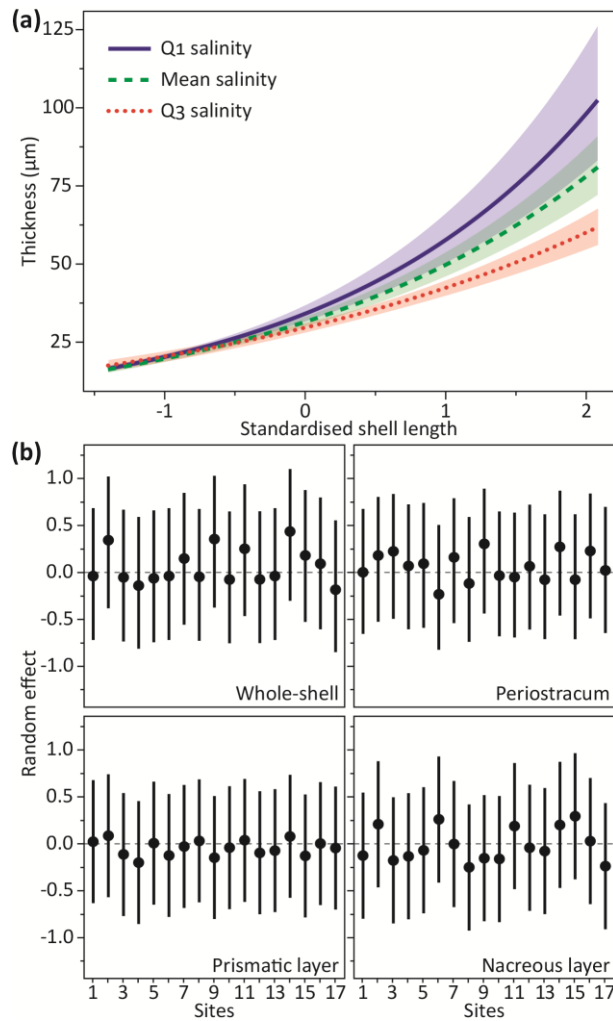
852 $-7.10, p < 0.0001, \text{pseudo}R^2 = 0.40$). Predicted values (solid line) and confidence intervals
 853 (shaded area) were estimated for mussels of mean shell length (52 mm).



854

855 **Figure 4.** Environmental influence on shell production and composition. (a) Predicted multiple
 856 relationships between the thickness of prismatic (solid margin plane) and nacreous (dashed
 857 margin plane) layers, and standardised salinity [mean (SD) = 25.52 psu (10.29)], shell length
 858 [mean (SD) = 47.42 mm (16.20)] and their interactions. (b) Shell thickness is modelled as a
 859 function of salinity for the 1st quartile ($Q_1 = 31.50$ mm), mean value (47.42 mm) and 3rd quartile
 860 ($Q_3 = 63.90$ mm) of the shell lengths sampled. For medium-sized mussels, we detected a

861 decreasing proportion of the prismatic layer (calcite) with increasing salinity and the deposition
862 of relatively thicker nacreous layers (aragonite) at salinities > 27.67 psu. (c) Thickness is
863 modelled as a function of length for the 1st quartile ($Q_1 = 18.92$ psu), mean value (25.52 psu)
864 and 3rd quartile ($Q_3 = 33.13$ psu) of salinity. At mean salinity, we detected an inversion of the
865 relative layers' thickness for shell length > 55.30 mm. Across the entire range of shell lengths,
866 the model predicts formation of prismatic layer-dominated shells under low salinities and
867 nacreous layer-dominated shells under higher salinities. Mean values (lines) and confidence
868 intervals (shaded areas) are predicted while controlling for temperature (13.03 °C) and Chl-*a*
869 (2.48 mg m⁻³).
870



871

872 **Figure 5. (a)** Interacting effects of salinity and shell length on periostracum. Periostracum

873 thickness is modelled as a function of standardised shell length [mean (SD) = 47.42 mm (16.20)]

874 for the 1st quartile ($Q_1 = 18.92$ psu, solid line), mean (25.52 psu, dashed line) and 3rd quartile

875 ($Q_3 = 33.13$ psu, dotted line) of water salinity. Predicted values (lines) and confidence intervals

876 (shaded areas) indicate higher rates of exponential periostracal thickening with decreasing

877 salinity. Smaller individuals (shell length < 48.38 mm) were characterised by non-significant

878 thickness differences under different salinity regimes. **(b)** Among sites shell variation. GLMMs'

879 conditional modes (filled circles) and variances (solid lines) of the random effect estimated for

880 individual shell layers. Modes represent the difference between the average predicted response

881 (layer thickness) for a given set of fixed-effects values (mean environmental covariates and shell
882 length) and the response predicted at a particular site. These suggest no detectable residual effect
883 of species (*Mytilus edulis* or *M. trossulus*) and level of hybridisation on shell thickness among
884 sites.

885